

Pumping of Confined Water in Carbon Nanotubes by Rotation-Translation Coupling

Sony Joseph and N. R. Aluru*

*Department of Mechanical Science and Engineering, Beckman Institute for Advanced Science and Technology,
University of Illinois at Urbana-Champaign, Urbana, Illinois 61801, USA*

(Received 1 August 2007; revised manuscript received 16 June 2008; published 6 August 2008)

Bidirectional single file water transport in a carbon nanotube is known to occur in “bursts” in short nanotubes. Here we show that in long carbon nanotubes, when the orientation of the water molecules is maintained along one direction, a net water transport along that direction can be attained due to coupling between rotational and translational motions. The rotations of the water molecules are correlated more with the translation of the neighboring water molecule with the acceptor oxygen than the neighbor with the donor hydrogen. This mechanism can be used to pump water through nanotubes.

DOI: 10.1103/PhysRevLett.101.064502

PACS numbers: 47.61.-k, 68.15.+e, 81.07.De

A rare combination of molecularly smooth walls and hydrophobicity of the surface make carbon nanotube (CNT) membranes a promising technology for drug delivery, selective ion transport, desalination, nanofiltration, etc. Water transport in carbon nanotubes has attracted considerable attention over the years [1–5]. Though bidirectional single file water transport in “bursts” through a (6, 6) CNT [1] and collective intermittent reversing of water dipolar orientations has been observed in molecular dynamics (MD) simulation for short tubes, the molecular mechanism governing the relation between the dipole orientation and the flow direction has not been elucidated. In this Letter, using molecular dynamics, we examine the molecular level mechanism of transport of confined water through finite length CNTs when the orientations are maintained along one direction. The orientations can be maintained by applying an electric field or by attaching chemical functional groups at the tube ends. The interaction of a uniform external electric field with molecules with net zero charge is through the torques, which are exerted only on the rotational degrees of freedom of the molecules. Any change in the translational degrees of freedom in such a system is to be attributed to the mechanism of coupling between rotational and translational motions.

For the molecular dynamics simulations, the system consisted of water molecules in a 9.83 nm long CNT attached to a bath of size $3.2 \times 3.2 \times 1.6 \text{ nm}^3$ at both ends of the tube. Semiconducting CNTs of two different diameters of 12.53 Å (16, 0) and 7.83 Å (10, 0) were considered. The CNT was modeled as Lennard-Jones atoms with parameters from Ref. [6]. Water was modeled using the single point charge/extended model. Simulations comparing polarizable models for CNTs with nonpolarizable models do not show any appreciable difference for water transport in semiconducting CNTs [7]. MD simulations were performed with GROMACS 3.3.2 [8], using a time step of 1 fs. The temperature of the fluid was maintained at 300 K by using a Nose-Hoover thermostat, and the pressure was kept at 1 bar using an anisotropic Parrinello-Rahman barostat with compressibility along the Z direction. Periodic boundary conditions were applied along X,

Y, and Z directions. The long-range electrostatic interactions were computed by using a particle mesh Ewald (PME) method, and the short-range interactions were computed using a cutoff scheme. Three different external electric field strengths ($E_{\text{ext}} = 0, 0.1, \text{ and } 1 \text{ V/nm}$) were applied along the channel in the $+ve$ Z direction. To consider the effect of screening by the CNT, an additional case was considered where the field was screened inside the CNT ($E_{\text{NT}} = E_{\text{ext}}/\epsilon$) by using a dielectric constant ϵ . For an infinitely long $(3n + 1, 0)$ CNT, $\epsilon = 30$ [9], but, adjusting for a finite length assuming a similar trend as in Ref. [10], we used an estimate of $\epsilon = 24$.

Figure 1 shows the cumulative flux of water molecules passing through (10, 0) and (16, 0) tubes for the different

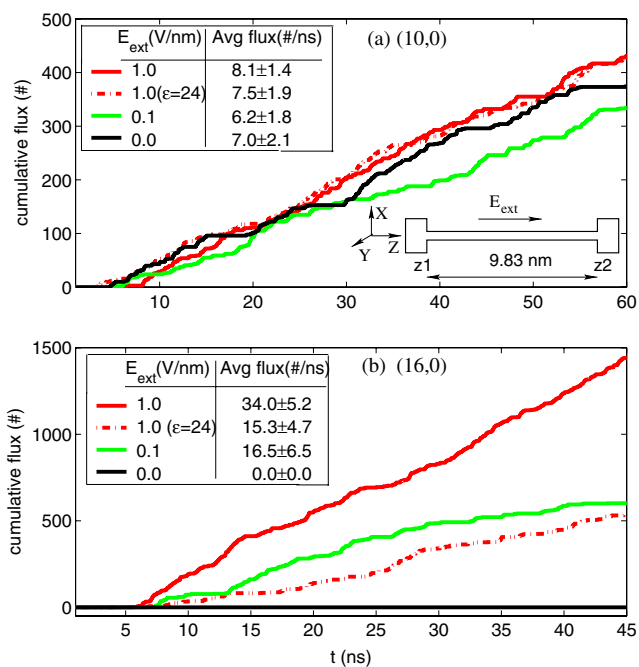


FIG. 1 (color online). The cumulative flux of water molecules crossing the tube as a function of time for (a) (10, 0) and (b) (16, 0) CNTs for various values of E_{ext} .

E_{ext} cases considered. The cumulative flux at time t is defined as the total number of water molecules that have crossed one end of the tube that had previously entered through the other end. It is defined as $+ve$ in the Z direction. The average fluxes computed by averaging the gradient of the cumulative flux in 10 ns intervals starting from $t = 10$ ns are also shown. We observe that (1) for the (10, 0) tube, the average water flux is similar regardless of the E_{ext} or screening effects, and (2) for the (16, 0) tube, higher $+ve$ average fluxes are present when the applied field is strong but decreases as the field decreases and screening effects are included. The average flux in an aquaporin channel ranges from 1–10 molecules/ns [11]. The (10, 0) tube has a single file water structure, and the (16, 0) tube has a structure with six files of water arranged in a hexagonal ring. During the entire simulation time, the direction of water dipoles was maintained in the $+ve Z$ direction for the (10, 0) tube regardless of the field, but for the (16, 0) tube the orientation along the $+ve Z$ direction was maintained only when the field was applied. The mean dipole orientation with respect to the $+ve Z$ axis $\langle \cos\theta \rangle$, where θ is the angle between the positive Z axis and the water dipole vector, averaged over all water molecules in the tube over the entire simulation time, was 0.83, 0.81, 0.74, and 0.00, for the (10, 0) CNT with $E = 1$ V/nm, the (10, 0) CNT with $E = 0$ V/nm, the (16, 0) CNT with $E = 1$ V/nm, and the (16, 0) CNT with $E = 0$ V/nm cases, respectively. The net transport is clearly in the direction of the aligned water dipoles. Single file water molecules are known to preferentially orient along one direction and intermittently reverse their orientations collectively in time scales of 4–6 ns for short 1.3 nm CNTs [1,6]. For the 9.83 nm long (10, 0) CNT with $E = 0$ V/nm case, the orientations have not reversed their direction from the initial orientation even after 60 ns. It is to be expected that at longer time scales flipping would cause the orientation to reverse for this case, so that there is a reversal in the direction of flow and there is no perpetual motion without any work being done. The time scales for flipping can be expected to be much longer for a 9.83 nm single file chain because of greater energy required to overcome a stronger cooperative hydrogen bond chain.

To understand the water fluxes, we analyze the flux in a (10, 0) tube and then examine the differences as the tube diameter increases. Figure 2(a) shows a 1.9 ps long trajectory smoothed over a 0.1 ps window for water molecules in the (10, 0) ($E = 0$ V/nm) CNT. The thick ball and stick models represent water molecules at the start of the trajectory, and lines of the same color represent the trajectory of each water molecule at intervals of 0.02 ps. A schematic of the single water file is also shown in Fig. 2(b). The neighboring water molecules undergo correlated rotational motions such that the resultant trajectory has a helical screwlike oscillatory motion. Note that the water dipoles are not strictly aligned to the $+ve Z$ direction, but the

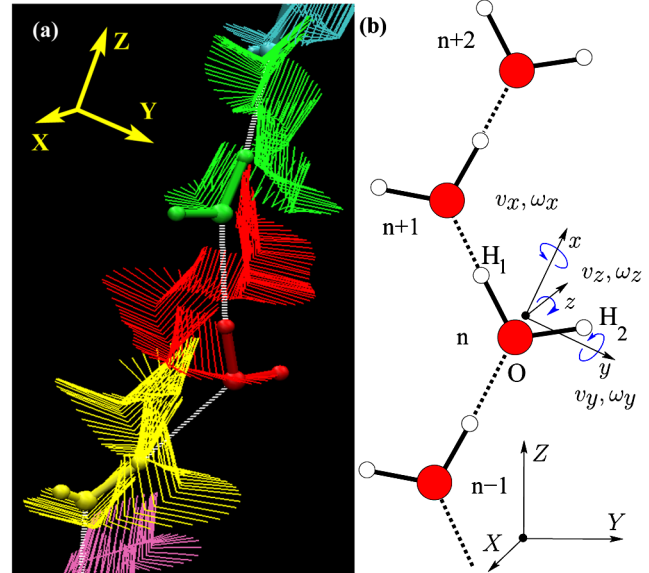


FIG. 2 (color online). (a) Trajectory of water molecules in a (10, 0) ($E = 0$ V/nm) CNT. Each color represents a water molecule's trajectory for 1.9 ps. The ball-stick models (various colors) denote the position of water at $t = 0$. (b) Schematic of a single file water with body centered principal axes frame xyz and the fixed box reference frame XYZ .

hydrogen-bonded OH vector [O-H₁ in Fig. 2(b)] of the n th water molecule is aligned with the dipole of the $(n + 1)$ th water molecule so as to minimize the energy of interaction with the neighboring molecules. As the relative distance between neighboring molecules changes, they undergo rotational motions as well as transfer linear momentum between them. In bulk water, these restricted rotational motions known as librations do not cause any net translational motion. In a long single file (10, 0) tube, or in the (16, 0) tube with electric field, under confinement, the characteristics of the librational motions could be different, and rotational-translational coupling (RTC) could give rise to a net transport.

To understand the restricted rotational motions of single file water, we analyze in Fig. 3 the velocity, angular velocity autocorrelation functions (ACFs), and their cross-correlation functions (CCFs) for water molecules in the (10, 0) CNT and in the bath in the xyz -principal axes [Fig. 2(b)] coordinate system where the moment of inertia tensor is diagonal. The x axis is in the direction of the dipole, the y axis is in the direction H₁ to H₂, and parallel to H₁-H₂, where H₁ is the hydrogen with a larger Z coordinate, and the z axis is out of the H₁-O-H₂ plane normal to the x and y axes. The velocity of a water molecule in a moving frame xyz can be related to the simulation box frame XYZ by three sets of direction cosines: $v_i = \sum_j R_{ij} V_j^b$, where $j = X, Y, Z$ are the simulation box axes, $i = x, y, z$ are the moving frame axes, v_i is the i th component of the velocity vector \mathbf{v} in the moving frame, and V_j^b is

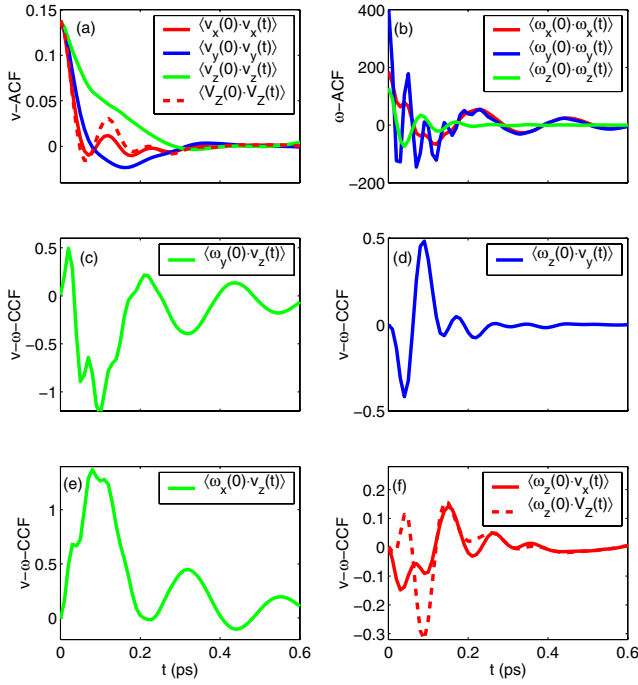


FIG. 3 (color online). Velocity autocorrelations $[(\text{nm}/\text{ps})^2]$, angular velocity autocorrelations $[(\text{rad}/\text{ps})^2]$, and nonvanishing velocity-angular velocity cross correlations $(\text{nm}/\text{ps} \cdot \text{rad}/\text{ps})$ for water molecules inside a (10, 0) tube for $E = 0$ V/nm.

the j th component of the simulation box velocity vector \mathbf{V}^b . The R_{ij} 's are the components of the rotation matrix made up of the direction cosines. The velocity autocorrelation function (v -ACF) can be written as $\langle v_i(t)v_i(0) \rangle = \langle \sum_j R_{ij}(t)V_j^b(t) \sum_k R_{ik}(0)V_k^b(0) \rangle$ [Fig. 3(a)]. Along with the v -ACFs along the three principal axes, also shown is the v -ACF along the axial Z direction of the tube [dashed red line in Fig. 3(a)]. Note that the x component of the v -ACF is the one that is the closest to the v -ACF along Z , which shows that the biggest contribution to the axial Z velocity is from that along the x direction. The components ω_i of the angular velocity vector $\boldsymbol{\omega}$ in the principal frame can be obtained by solving $\boldsymbol{\omega} = \mathbf{I}^{-1}\mathbf{L}$, where $\mathbf{L} = \sum_l m_l(\mathbf{r}_l \times \mathbf{v}_l)$ is the angular momentum vector about the center of mass in the principal axes reference frame, $l = \text{O}, \text{H}_1, \text{H}_2$, \mathbf{r}_l is the coordinate vector of atom l in the principal axis reference frame whose origin is at the center of mass, m_l is the mass of atom l , \mathbf{I} is the moment of inertia tensor in the principal axes frame with nonzero diagonal elements computed as $I^{ii} = \sum_l m_l(r_l^i)^2$, $i = x, y, z$, and r_l^i 's are the x , y , and z coordinates in the principal axis reference frame. The angular velocity autocorrelation (ω -ACF) is defined as $\langle \omega_i(t)\omega_i(0) \rangle$, and the cross correlation (v - ω -CCF) is defined as $\langle v_i(t)\omega_h(0) \rangle$, where $i = h = x, y, z$. In Fig. 3(b), the ACFs of ω_x and ω_y have similar characteristics with a superposition of a high frequency mode and a low frequency mode that decays much slower. Note that ω_z has a different frequency of oscillation than ω_x and ω_y .

Figures 3(c)–3(f) show the four nonzero CCFs that indicate coupling between rotational and translational motions. Also shown is the only nonzero CCF between the angular velocity and the box frame velocity $\langle \omega_z(0)V_Z(t) \rangle$ [Fig. 3(f)]. From Figs. 3(c) and 3(e), it is seen that linear combination of a $+ve \omega_x$ and a $-ve \omega_y$ can be coupled to a $+ve v_z$ (or $+ve \omega_y$ and $-ve \omega_x$ coupled to $-ve v_z$) that give rise to out-of- H_1OH_2 -plane helical motions [Fig. 2(a)]. The rotation ω_z can be coupled to velocities v_x and v_y [Figs. 3(d) and 3(f)]. Of all the rotations ω_x , ω_y , and ω_z , the one that gives a net translation along the Z direction is ω_z , as the only nonzero CCF between angular velocities and box frame velocities is $\langle \omega_z(0)V_Z(t) \rangle$ [Fig. 3(f)]. From the v -ACF in Fig. 3(a), the v -ACF closest to the v -ACF of V_Z is that of v_x , and the biggest contribution to net axial velocity from RTC is $\langle \omega_z(0)v_x(t) \rangle$. Figure 4 has the cross correlations of $\langle \omega_z(0)v_x(t) \rangle$ for (16, 0) tubes with and without an electric field and in the bath. As the field strength decreases to zero, the coupling diminishes in the (16, 0) tube, and no net flux is generated in 45 ns, since orientations are not maintained. In the bath, the coupling $\langle \omega_z(0)v_x(t) \rangle$ is zero.

In the previous paragraph, we discussed the coupling of the rotation of one molecule about its center of mass to its translational velocity. In order to understand the coupling between the rotation of one molecule and the translation of the neighboring molecules, and to distinguish between net translation in the $+ve Z$ direction and in the $-ve Z$ direction, we plot the CCFs between the n th and the $(n \pm j)$ th molecules where $j = -2, -1, 1, 2$ for the (10, 0) tube. $(n + 1)$ is the neighboring molecule with the acceptor oxygen, and $(n - 1)$ is the neighboring molecule with the donor hydrogen [Fig. 2(b)]. Figure 5(a) shows the CCF between the axial velocities, and Fig. 5(b) has the CCF between the angular velocity of a molecule and the axial velocity of the neighboring molecule. From Fig. 5(a), it is

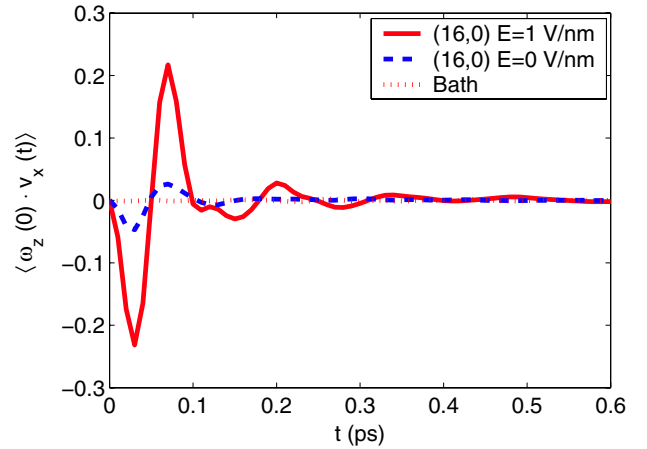


FIG. 4 (color online). Cross correlations of angular velocity ω_z with v_x for (16, 0) tubes for $E = 1$ V/nm, $E = 0$ V/nm, and in the bath.

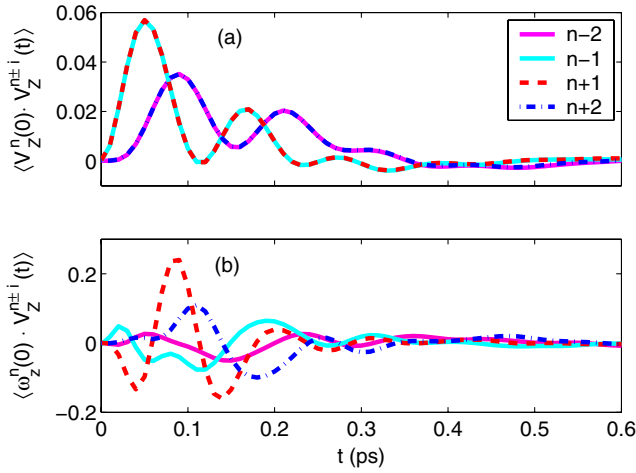


FIG. 5 (color online). (a) Cross correlation of the axial velocity of the neighboring ($n \pm i$)th water molecule with axial velocity of the n th water molecule for the (10, 0) tube. (b) Cross correlation of the axial velocity of the neighboring ($n \pm i$)th water molecule with the out-of-plane angular velocity ω_z of the n th water molecule. Coupling with ($n + 1$) and ($n + 2$) are greater than that with ($n - 1$) and ($n - 2$) showing preferred transfer of rotational energy to translational energy along the $+ve$ Z direction.

seen that the CCF $\langle V_Z^n(0)V_Z^{n+1}(t) \rangle$ is the same as $\langle V_Z^n(0)V_Z^{n-1}(t) \rangle$ and likewise for the CCFs $\langle V_Z^n(0)V_Z^{n+2}(t) \rangle$ and $\langle V_Z^n(0)V_Z^{n-2}(t) \rangle$. If the profiles for $n \pm 2$ are shifted to the left by $\Delta t = 0.05$ ps, the locations of the peaks and valleys match, suggesting a collision time of 0.05 ps between neighbors. The linear momentum transfer between the neighboring molecules is the same in both directions. But in Fig. 5(b), the cross correlations between the rotations of the n th and the axial velocity of ($n + 1$)th shows a stronger correlation than that between the n th and the ($n - 1$)th water molecule. The same trend is observed for ($n + 2$)th and ($n - 2$)th molecules. The CCF $\langle \omega_z^n(0)V_Z^{n+2}(t) \rangle$ has similar features as $\langle \omega_z^n(0)V_Z^{n+1}(t) \rangle$ with a shift of $\Delta t = 0.05$ ps. This shows a preferential transfer of rotational energy of the n th molecule towards the translation of ($n + 1$)th and ($n + 2$)th molecules as compared to the opposite direction.

To check whether the phenomenon was caused by periodicity in the Z direction, even with baths attached, we performed NVT simulations with sufficient empty space beyond the 4 nm long baths. Periodicity was applied only along the X and Y directions using a 2D corrected PME [8]. We found that fluxes were in the direction of the electric field ($E_{\text{ext}} = 0.01, 0.1, \text{ and } 1$ V/nm), and the same ACFs and CCFs as seen previously were obtained. For the (10, 0) tube with $E_{\text{ext}} = 0$ V/nm, the orientation flipped 3 times in

60 ns, and fluxes in both directions were obtained depending on the direction of the orientation.

In order to ascertain whether this phenomenon is not a result of entrance-exit effects, we also performed simulations with infinitely long periodic tubes without baths at the ends. The fluxes generated were in the direction of the dipoles with the same correlations.

The cumulative fluxes do not increase uniformly with time but in bursts in the (10, 0) tube [Fig. 1(a)]. The variations in the fluxes are related to the fluctuations in the occupancy of water in the tube [37–40 in the (10, 0) tube] from the fully filled state. At the highest occupancy, the number of cooperative hydrogen bonds in the tube is maximum, but, as occupancy decreases from the maximum value, the hydrogen bond chain is broken and the increase in cumulative flux is slower.

To maintain orientations without a large E_{ext} , asymmetric functional groups can be attached at the ends [12]. With chemical functionalization, the mechanism of water transport by RTC could pave the way towards developing ultra-efficient, next-generation nanofluidic devices.

This work was supported by NSF under Grants No. 0120978 (Water CAMPWS, UIUC), No. 0325344, No. 0328162 (nano-CEMMS, UIUC), and No. 0523435 and by NIH under Grant No. PHS 2 PN2 EY016570B.

*Corresponding author.

aluru@uiuc.edu; <http://www.uiuc.edu/~aluru>

- [1] G. Hummer, J. Rasaiah, and J. Noworyta, *Nature (London)* **414**, 188 (2001).
- [2] M. Majumder, N. Chopra, R. Andrews, and B. Hinds, *Nature (London)* **438**, 44 (2005).
- [3] J. K. Holt, H. G. Park, Y. Wang, M. Stadermann, A. B. Artyukhin, C. P. Grigoropoulos, A. Noy, and O. Bakajin, *Science* **312**, 1034 (2006).
- [4] M. Whitby and N. Quirke, *Nature Nanotech.* **2**, 87 (2007).
- [5] S. Joseph and N. Aluru, *Nano Lett.* **8**, 452 (2008).
- [6] C. Y. Won, S. Joseph, and N. R. Aluru, *J. Chem. Phys.* **125**, 114701 (2006).
- [7] F. Moulin, M. Devel, and S. Picaud, *Phys. Rev. B* **71**, 165401 (2005).
- [8] E. Lindahl, B. Hess, and D. van der Spoel, *J. Mol. Model.* **7**, 306 (2001).
- [9] B. Kozinsky and N. Marzari, *Phys. Rev. Lett.* **96**, 166801 (2006).
- [10] D. Lu, Y. Li, S. Rotkin, U. Ravaioli, and K. Schulten, *Nano Lett.* **4**, 2383 (2004).
- [11] J. B. Heymann and A. Engel, *News Physiol. Sci.* **14**, 187 (1999).
- [12] S. Joseph, R. J. Mashl, E. Jakobsson, and N. R. Aluru, *Nano Lett.* **3**, 1399 (2003).